Neoadjuvant Chemotherapy and Immunotherapy in Luminal B-like Breast Cancer: Results of the Phase II GIADA Trial

Maria Vittoria Dieci[1,2], Valentina Guarneri[1,2], Anna Tosi[1], Giancarlo Bisagni[3], Antonino Musolino[4,5], Simon Spazzapan[6], Gabriella Moretti[3], Grazia Maria Vernaci[1,2], Gaia Griguolo[1,2], Tommaso Giarratano[2], Loredana Urso[1], Francesca Schiavi[7], Claudia Pinato[7], Giovanna Magni[8], Marcello Lo Mele[9], Gian Luca De Salvo[8], Antonio Rosato[1,10], and Pierfranco Conte[1,2]

ABSTRACT

Purpose: The role of immunotherapy in hormone receptor (HR)-positive, HER2-negative breast cancer is underexplored.

Patients and Methods: The neoadjuvant phase II GIADA trial (NCT04659551, EUDRACT 2016-004665-10) enrolled stage II–IIIA premenopausal patients with Luminal B (LumB)-like breast cancer (HR-positive/HER2-negative, Ki67 ≥ 20%, and/or histologic grade 3). Patients received: three 21-day cycles of epirubicin/cyclophosphamide followed by eight 14-day cycles of nivolumab, triptorelin started concomitantly to chemotherapy, and exemestane started concomitantly to nivolumab. Primary endpoint was pathologic complete response (pCR; ypT0/is, ypN0).

Results: A pCR was achieved by 7/43 patients [16.3%; 95% confidence interval (CI), 7.4–34.9]; the rate of residual cancer burden class 0–I was 25.6%. pCR rate was significantly higher for patients with PAM50 Basal breast cancer (4/8, 50%) as compared with other subtypes (LumA 9.1%; LumB 8.3%; $P = 0.017$). Tumor-infiltrating lymphocytes (TIL), immune-related gene-expression signatures, and specific immune cell subpopulations by multiplex immunofluorescence were significantly associated with pCR. A combined score of Basal subtype and TILs had an AUC of 0.95 (95% CI, 0.89–1.00) for pCR prediction. According to multiplex immunofluorescence, a switch to a more immune-activated tumor microenvironment occurred following exposure to anthracyclines. Most common grade ≥3 treatment-related adverse events (AE) during nivolumab were γ-glutamyltransferase (16.7%), alanine aminotransferase (16.7%), and aspartate aminotransferase (9.5%) increase. Most common immune-related AEs were endocrinopathies (all grades 1–2; including adrenal insufficiency, $n = 1$).

Conclusions: Luminal B-like breast cancers with a Basal molecular subtype and/or a state of immune activation may respond to sequential anthracyclines and anti–PD-1. Our data generate hypotheses that, if validated, could guide immunotherapy development in this context.

Introduction

Hormone receptor (HR)-positive, HER2-negative breast cancer accounts for 70% of invasive breast cancers. Molecular and pathology-based approaches have contributed to dissect its heterogeneity. The subclassification as Luminal A-like (LumA-like) or Luminal B-like (LumB-like) by immunohistochemistry (IHC) recapitulates, even though not completely overlapping, the molecular intrinsic subtypes and is currently used in clinical practice. As compared with LumA-like, LumB-like tumors show higher proliferation, lower expression of progesterone receptor, and are associated with a higher cumulative incidence of distant metastasis (up to 24.5% at 10 years; refs. 1, 2). Due to this increased risk of relapse, the systemic treatment for early LumB-like breast cancer patients frequently includes both chemotherapy and endocrine therapy (2).

The neoadjuvant setting is ideal to test new treatment strategies, evaluate their efficacy according to biological heterogeneity, and assess their effect on biomarkers. Chemotherapy is nowadays the standard systemic option for premenopausal HR-positive, HER2-negative breast cancer patients who are candidate to a neoadjuvant strategy (2). The achievement of a pathologic complete response (pCR) after neoadjuvant chemotherapy is associated with improved long-term outcome across all breast cancer subtypes (3). Among HR-positive, HER2-negative patients, the association between pCR and prognosis is more evident for LumB-like than LumA-like tumors (4). Nevertheless, the pCR rate for LumB-like breast cancer patients remains low even with modern regimens (approximately 10%; ref. 5).

[1]Department of Surgery, Oncology and Gastroenterology, University of Padova, Padova, Italy. [2]Medical Oncology 2, Veneto Institute of Oncology IOV-IRCCS, Padova, Italy. [3]Department of Oncology and Advanced Technologies, Oncology Unit, Azienda USL-IRCCS, Reggio Emilia, Italy. [4]Medical Oncology and Breast Unit, University Hospital of Parma, Parma, Italy. [5]Department of Medicine and Surgery, University of Parma, Parma, Italy. [6]Department of Medical Oncology, Centro di Riferimento Oncologico di Aviano (CRO) IRCCS, Aviano, Italy. [7]UOSD Hereditary Tumors, Veneto Institute of Oncology IOV-IRCCS, Padova, Italy. [8]Clinical Research Unit, Veneto Institute of Oncology IOV-IRCCS, Padova, Italy. [9]Department of Pathology, Azienda Ospedale Università Padova, Padova, Italy. [10]Immunology and Molecular Oncology Diagnostics, Veneto Institute of Oncology IOV-IRCCS, Padova, Italy.

M.V. Dieci and V. Guarneri contributed equally as first author.

A. Rosato and P. Conte contributed equally as last author.

Corresponding Author: Maria Vittoria Dieci, Department of Surgery, Oncology and Gastroenterology - University of Padova, Division of Medical Oncology 2, Veneto Institute of Oncology IOV-IRCCS, Via Gattamelata 64, 35128, Padova, Italy. Phone: 3904-9821-5295; Fax: 3904-9821-5932; E-mail: mariavittoria.dieci@unipd.it

Clin Cancer Res 2022;28:308–17

doi: 10.1158/1078-0432.CCR-21-2260

Translational Relevance

Hormone receptor (HR)-positive/HER2-negative breast cancer is generally considered a cold tumor. We report the first neoadjuvant trial of immunotherapy specifically dedicated to patients with HR-positive/HER2-negative Luminal B-like breast cancer. Sequential anthracycline-based chemotherapy followed by nivolumab and endocrine therapy induced a 16.3% pathologic complete response (pCR) rate. Although the primary endpoint was not met, extensive molecular and immune characterization by multiplex immunofluorescence allowed the identification of immune-related gene signatures (CD8 T cells, cytotoxic cells, cytotoxicity, IFN gamma, inflammatory chemokines, macrophages, PD-L1, PD-L2, IDO-1, TIGIT, and tumor inflammation signature) and immune cell subpopulations associated with pCR. A combined score of tumor-infiltrating lymphocytes and Basal molecular subtype showed an AUC of 0.95 for pCR prediction. Our results provide unique insights that contribute to change the way HR-positive/HER2-negative breast cancer is considered from an immunogenic perspective and provide novel hints to trace the path of immunotherapy development in this disease.

Immune-checkpoint inhibitors are gaining momentum in the treatment of breast cancer (6–8). HR-positive, HER2-negative breast cancer is considered the least immunogenic of all breast cancers, being characterized by low levels of tumor-infiltrating lymphocytes (TIL) and low tumor mutational load. For these reasons, the role of immunotherapy in this condition has been underexplored (9). Notwithstanding, LumB-like tumors may present immunogenic features that could promote sensitivity to immunotherapy, such as higher TILs and tumor mutational burden as compared with LumA-like, and the expression of immune checkpoints (10–12).

Anthracyclines, as potent inducers of immunogenic cell death, are particularly attractive as a priming strategy to turn the tumor immune microenvironment toward an antitumor state that can ease the activity of immune-checkpoint inhibitors (13–14). Multiple studies have demonstrated that estrogens show pleotropic effects on immune cells generally favoring tumor progression and that aromatase inhibitors and/or ovarian function suppression promote an antitumor immune microenvironment, delineating the biological rationale for combining immunotherapy with endocrine treatment (9, 15, 16).

On these premises, we conducted the phase II neoadjuvant GIADA trial to test the hypothesis that a neoadjuvant treatment with anthracycline-based chemotherapy followed by anti–PD-1 immunotherapy in combination with endocrine treatment is effective for premenopausal LumB-like breast cancer patients.

Patients and Methods

Study design and participants

GIADA is an investigator-driven, phase II, single-arm, multicentric trial conducted at four Italian institutions (NCT04659551, EUDRACT 2016-004665-10). Eligible patients were premenopausal women (≥18 years) with newly diagnosed, previously untreated, histologically confirmed LumB-like invasive breast cancer. LumB-like was defined according to local pathology as HR positive (estrogen receptor and/or progesterone receptor expression in ≥10% of tumor cells by IHC), HER2 negative (according to the American Society of Clinical Oncology and College of American Pathologists guidelines), with high Ki67 (≥20% by IHC) and/or histologic grade 3. Patients had stage II to IIIA breast cancer and were candidate to neoadjuvant chemotherapy based on local multidisciplinary evaluation. Other key inclusion criteria were: Eastern Cooperative Oncology Group performance status 0–1 and normal bone marrow, liver, and renal function. Key exclusion criteria included: stage IIIB, IIIC, IV, and inflammatory breast cancer; contraindication to anthracyclines; and other common exclusion criteria in immunotherapy trials. The study was conducted according to Good Clinical Practice Guidelines and the World Medical Association Declaration of Helsinki. All patients provided written informed consent. The trial protocol and all amendments were approved by the competent ethical committee at each participating institution.

Procedures

Eligible patients received three 21-day cycles of intravenous epirubicin 90 mg/m^2 and cyclophosphamide 600 mg/m^2, followed by eight 14-day cycles of intravenous nivolumab 240 mg. Oral exemestane 25 mg daily was started concomitant to nivolumab, and intramuscular triptorelin 3.75 mg every 28 days was started concomitant to chemotherapy. Endocrine therapy was maintained until surgery. Patients underwent surgery 2 to 5 weeks from the last nivolumab dose. Adjuvant therapy was at physician's discretion. Study design is represented in Supplementary Fig. S1.

At baseline, patients underwent radiologic tumor assessment by mammogram and ultrasound, physical examination, routine work-up staging, vital signs assessment, laboratory tests, and 12-lead electrocardiogram. The type of surgery indicated in the absence of neoadjuvant treatment was collected at baseline. Laboratory tests, vital signs, and physical examination were assessed at every chemotherapy and nivolumab cycle, and before surgery. Prior to surgery, tumor measurement by mammogram and ultrasound was performed. Adverse events were assessed by the Common Terminology Criteria for Adverse Events, version 4.03.

Formalin-fixed paraffin-embedded (FFPE) tumor tissue specimens were collected at baseline (core biopsy, t0), after chemotherapy within 7 days prior to the first nivolumab dose (core biopsy, t1), and at surgery (surgical sample, t2). Fresh-frozen samples from diagnostic core biopsies were also centralized.

Outcomes

The primary endpoint was the rate of patients achieving a pCR by local pathology evaluation, defined as the absence of invasive cancer cells in breast and axilla (ypT0/is, ypN0).

Key secondary endpoints reported here are clinical objective responses in the breast, safety, breast conservative surgery rate, conversion from mastectomy, molecular intrinsic subtypes by PAM50, gene-expression, and immune-related tissue biomarkers.

Clinical objective responses in the breast were defined as partial or complete responses according to the Modified Response Evaluation Criteria in Solid Tumors (version 1.1), based on ultrasound examination performed at baseline and immediately before surgery.

The rate of breast conservative surgery was calculated as the percentage of conservative procedures over total surgeries. The conversion from mastectomy was calculated as the percentage of patients initially candidate to mastectomy who underwent breast conserving surgery.

Gene-expression analyses

Fresh-frozen baseline tumor biopsies were reviewed by a pathologist for tumor tissue quality and quantity. All the biopsies contained at least 40% of tumor cells.

Frozen tumor tissues were disrupted in liquid nitrogen using a mortar and pestle. Ground tissues were resuspended in lysis buffer, RTL buffer (Qiagen) plus β-mercaptoethanol, and homogenized by passing the lysate at least five times through a 20-gauge needle. Total RNA was extracted using the RNeasy Plus mini kit (Qiagen) following the manufacturer's instructions.

If fresh-frozen tumor biopsy were not available, FFPE baseline tumor biopsies were evaluated by a pathologist for tumor tissue quality and quantity. From each FFPE baseline tumor biopsy, five 10-μm sections were cut, and RNA was extracted using the RNeasy FFPE Kit (Qiagen) following the manufacturer' instructions.

RNA concentration and quality were assessed with Nanodrop 1000 Spectrophotometer (Thermo Scientific NanoDrop Products), Qubit RNA HS Assay Kit on Qubit fluorometer 1.0 (Invitrogen, Life Technologies), and TapeStation 4200 (Agilent Technologies, Germany) to ensure they met the specifications for purity (260/280 ratio between 1.7 and 2.3) and concentration (≥10 ng/μL).

RNA extracted from fresh-frozen or, if not available, FFPE tumor samples was used to measure the expression of 758 breast cancer–related genes and 18 housekeeping genes using the Breast Cancer 360 Panel on an nCounter platform (NanoString Technologies).

The samples were processed according to the manufacturer's instructions and kits provided by NanoString Technologies. Briefly, the starting material was 100 ng RNA for fresh-frozen tissue and 200 or 300 ng for FFPE samples depending on the percentage of fragments with dimensions greater than 200 bp (DV200 value). RNA concentration and quality were assessed with Nanodrop 1000 Spectrophotometer (Thermo Scientific NanoDrop Products) and Qubit RNA HS Assay Kit on Qubit fluorometer 1.0 (Invitrogen, Life Technologies) to ensure they met the specifications for purity (260/280 ratio between 1.7 and 2.3) and concentration (≥10 ng/μL). RIN and DV200 were evaluated with the High Sensitivity RNA kit on TapeStation 4200 (Agilent Technologies, Germany). Sample RNA was hybridized with panel probes for 17 hours at 65°C and then complexes were processed on the nCounter Analysis System. Cartridges were scanned at 555 FOVs.

The Breast Cancer 360TM assay covers genes from different independent signatures, including the PAM50 signature. The panel includes 758 target probe pairs, 18 housekeeping genes used for normalization, 6 exogenous positive control RNA targets that range linearly from 128 fM to 0.125 fM, and 8 exogenous negative control sequences. Zero counts on the raw scale are converted to ones prior to normalization.

Gene-expression data for genes nonincluded in the PAM50 or TIS (Tumor Inflammation Signature) signatures were normalized using a ratio of the expression value to the geometric mean of all housekeeping genes on the panel. Genes in the TIS signature were normalized using a ratio of the expression value to the geometric mean of the housekeeper genes used only for the TIS signature, whereas genes in the PAM50 signature were normalized using a ratio of the expression value to the geometric mean of the housekeeper genes used only for the PAM50 signature.

Genes not in the PAM50 signature were additionally normalized using a ratio of the housekeeper-normalized data and a panel standard run on the same cartridge or on the same codeset lot as the observed data.

Data were then Log2 transformed. Forty-eight gene signatures covering several aspects of breast cancer biology and predefined by the manufacturer for the Breast Cancer 360 Panel (NanoString Technologies) were calculated, including intrinsic molecular subtyping was determined using the previously reported PAM50 subtype predictor (17). Gene signatures were adapted with constants to make scores comparable across research-use only and investigational-use only assays.

Histology and multiplex fluorescence IHC (mIHC)

Immune-related biomarkers were evaluated on representative tumor samples (presence of infiltrating tumor cells confirmed by central pathology) collected at t0, t1, and t2.

Stromal TILs were evaluated on a hematoxylin and eosin–stained slide according to the International Tumor-Infiltrating Lymphocytes Working Group recommendations (18). Androgen receptor nuclear staining was evaluated on whole sections by IHC with the Dako AR441 antibody and reported as the percentage of positive cells.

mIHC analysis was carried out on sequential 4-μm-thick FFPE tumor tissue sections. Two staining panels were used: the "checkpoint panel" included primary antibodies against CD68 (clone KP1, Dako), CD163 (clone 10D6, Leica Biosystems), CD3 (clone F.7.2.38, Dako), PD-1 (clone EPR4877-2, Abcam), and PD-L1 (clone E1L3N, Cell Signaling Technology), whereas the "lymphoid panel" included antibodies against granzyme B (clone 11F1, Leica Biosystems), CD4 (clone 4B12, Thermo Fisher), CD8 (clone C8/144B, Dako), FoxP3 (clone D2W8E, Cell Signaling Technology), and CD20 (clone L26, Dako). In both panels, the anti–pan-cytokeratin antibody (clone AE1/AE3, Dako) was added as a tumor marker (Supplementary Fig. S2). Prior to staining, sections were deparaffinized in Clearene (Leica Biosystems) and rehydrated by serial passages in graded ethanol. A 20-minute passage in 10% neutral buffered formalin (Sigma) ensured the fixation of the sample on the glass slide.

Heat-induced epitope retrieval was performed with a microwave oven using a Target Retrieval Solution pH9 (Dako) or pH6 (Akoya Biosciences), depending on primary antibody. The staining procedure consisted of six sequential rounds, each including protein blocking with Protein Block Serum-free (Dako), followed by incubation with primary antibody and 10-minute incubation with an anti-mouse + rabbit horseradish peroxidase (HRP)-conjugated secondary antibody (Akoya Biosciences). Each marker was coupled with a different Tyramide Signal Amplification (TSA)-conjugated Opal fluorophore (Akoya Biosciences). After all six sequential reactions, slides were counterstained with spectral DAPI (Akoya Biosciences) and mounted using Vectashield Hardset mounting medium (Vector Labs).

Multiplex stained slides were scanned using the Mantra Quantitative Pathology Workstation (Akoya Biosciences) at 4× and 20× magnification. For each sample, only areas comprising tumor cells were considered. Multispectral images were unmixed using a spectral library built from images of single fluorophore-stained control tissues using the inForm Image Analysis software (version 2.4.9, Akoya Biosciences). A selection of representative multispectral images was used to train the inForm software in order to create an algorithm for each panel: tissue segmentation based on recognition of cytokeratin-positive cells; cell segmentation based on nuclear and membrane staining; and cell phenotyping based on the detection of cell-surface and intracellular markers. The created algorithms were applied in the batch analysis of all acquired seven-color multispectral images of the same panel, to examine the presence of tumor-infiltrating immune cells within the tumor area and in the surrounding stroma. Cell densities (cells/mm^2) were calculated for each patient as the mean of all acquired fields on the same tissue slide (at least 20 fields at 20× magnification for each stained slide). Cell densities were evaluated separately in the intratumoral and stromal compartments.

Statistical analysis

Sample size was estimated using a Simon two-stage design. Assuming a 10% pCR rate with standard chemotherapy, a pCR of 25% with the study treatment was considered of interest. Setting $\alpha = 0.05$ and $\beta = 0.20$, a total of 43 patients were required. The first stage (at least 3 pCR out of 18 patients) was accomplished in November 2018. In the second stage, an additional 25 patients were enrolled. To fulfill the statistical hypothesis, at least 8 pCR of 43 patients were required.

Efficacy endpoints were evaluated on the intention-to-treat population including all enrolled patients. Clinical objective response is reported for patients who underwent breast ultrasound both at baseline and immediately before surgery. Percentages and their 95% confidence intervals (95% CI) were calculated according to the Wilson method with continuity correction.

The incidence of treatment-related adverse events (TRAE; relation with study treatment determined by the physician) was calculated by treatment phase.

The association of molecular subtypes and TILs with pCR was studied using univariate logistic regression or the χ^2 test. The association of gene signatures with pCR was studied using a linear model without a blocking factor with *P* values adjusted using the Benjamini and Yekutieli false discovery rate adjustment (models fitted using the limma package in R).

Bivariate correlation between gene signatures was assessed by the Pearson coefficient. The Mann–Whitney *U* test was used to compare immune biomarkers between pCR and non-pCR patients. The Wilcoxon-signed rank test was used to study the modulation of biomarkers at different timepoints. Given their exploratory nature, analyses of immune-related tissue biomarkers were not adjusted for multiple testing (19).

The combined score of Basal subtype and TILs was calculated from the estimated coefficient of each variable in a bivariate logistic model for pCR: TILs (%) $\times$ 0.15 + Basal (0 = no, 1 = yes) $\times$ 2.37. The performance of the score was estimated by determining the area under the ROC curve (AUC).

The level of significance was $P < 0.05$. Data were analyzed with IBM SPSS Statistics (version 27), R software (version 4.0.3), and SAS (version 9.4; ref. 20).

Results

From October 2017 to October 2019, 45 patients were assessed for eligibility and 43 were enrolled (**Fig. 1**). All enrolled patients received at least one dose of study treatment and underwent surgery. Overall, 81.4% of patients received at least six courses of nivolumab. Nine patients permanently discontinued nivolumab for safety reasons (including grade 3 pancreatitis $n = 1$, grade 3 liver toxicity $n = 6$, grade 2 liver toxicity $n = 1$, grade 3 erythema nodosum $n = 1$), and 3 patients discontinued nivolumab for other reasons (including two with local progression). One patient permanently discontinued study treatment after the three courses of chemotherapy due to febrile neutropenia.

Patient characteristics are reported in **Table 1**. The majority (81.5%) presented with a clinical stage II breast cancer, 48.8% had no axillary node involvement, and most had a ductal breast cancer (95.3%). All patients met the LumB-like inclusion criteria: 95% had a HR-positive, HER2-negative tumor with Ki67 ≥20% (any histologic grade); $n = 2$ (5%) had a HR-positive, HER2-negative tumor with Ki67 <20% and histologic grade 3.

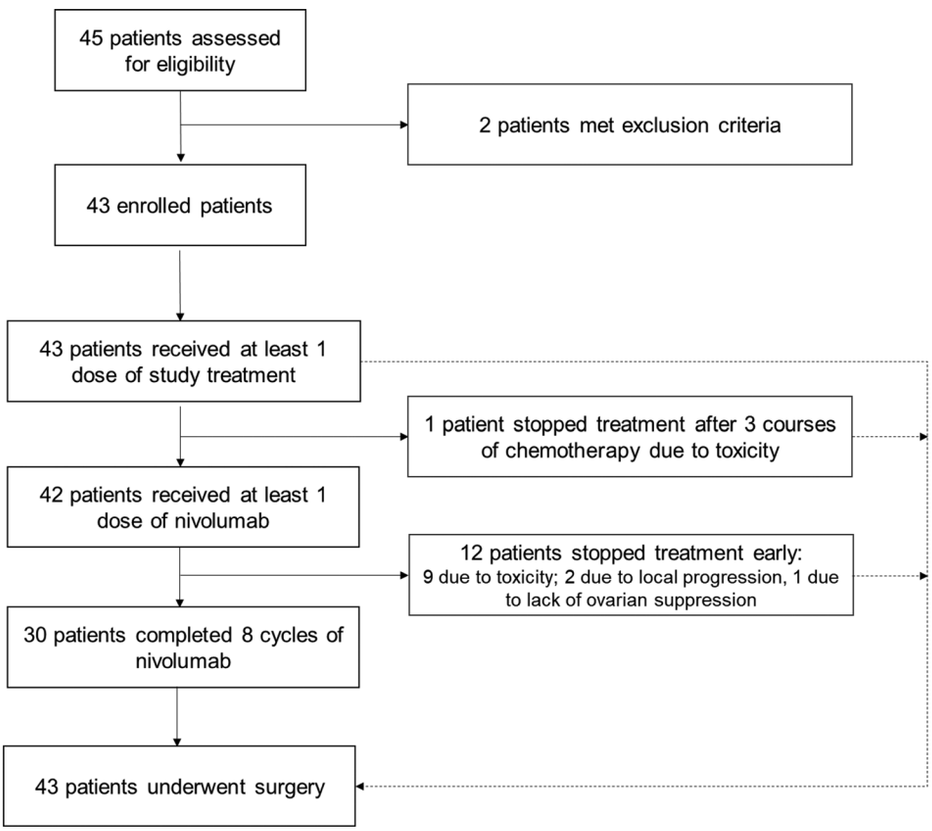

Figure 1.
CONSORT diagram.

Table 1. Patient baseline characteristics.

Characteristic		***N* = 43** ***n* (%)**
Age, years	Median (range)	45 (31–54)
Clinical stage	IIa	21 (48.9%)
	IIb	14 (32.6%)
	IIIa	8 (18.6%)
Tumor size	T1	4 (9.3%)
	T2	32 (74.4%)
	T3	7 (16.3%)
Lymph node status	N0	21 (48.8%)
	N1	18 (41.9%)
	N2	4 (9.3%)
Histologic type	Ductal	41 (95.3%)
	Lobular	2 (4.7%)
Histologic tumor grade	Grade 1	1 (2.3%)
	Grade 2	18 (41.9%)
	Grade 3	24 (55.8%)
ER expression	Median %, (Q1:Q3)	90 (75:95)
	≥10%	43 (100%)
PgR expression	Median % (Q1:Q3)	82.5 (40:90)
	≥10%	38 (88.4%)
Ki67, %	Median (Q1:Q3)	30 (25:41)
HER2 status	IHC 0/1+	29 (67.4%)
	IHC 2+ and FISH-neg	6 (14.0%)
	FISH-neg	8 (18.6%)
Phenotype	$HR^+/HER2^-$, Ki67 ≥ 20%, any grade	41 (95%)
	$HR^+/HER2^-$, Ki67 < 20%, grade 3[a]	2 (5%)

Abbreviations: ER, estrogen receptor; FISH, fluorescent *in situ* hybridization; HR, hormone receptor; IHC, immunohistochemistry; *N*, number; PgR, progesterone receptor; Q1, first quartile; Q3, third quartile; tot, total.

[a]These two patients had progesterone receptor expression >20%, thus not meeting the LumB-like definition according to the European Society of Medical Oncology guidelines (2).

Seven out of 43 patients achieved a pCR (16.3%; 95% CI, 7.4%–34.9%, not meeting the prespecified hypothesis; **Fig. 2A**) and 11 achieved a residual cancer burden class 0–I (25.6%; 95% CI, 14.0%–41.8%, endpoint not prespecified in the protocol, centrally evaluated; ref. 21). Thirty-four patients underwent ultrasound examination at baseline and before surgery, and 24 obtained a clinical objective response in the breast (70.6%; 95% CI, 52.3%–85.5%). Of the 34 patients evaluable for objective clinical response, 82.4% had a breast radiologic assessment that was concordant with the pathologic response ($n = 4$ complete response in the breast by ultrasound/yT0; $n = 24$ no complete response in the breast by ultrasound/no yT0). Thirteen patients underwent a breast conservative intervention (30.2%; 95% CI, 17.7%–46.7%). The type of surgery indicated at baseline was available for 38 patients. Of the 28 patients initially candidate to mastectomy, 7 underwent breast conservative surgery (conversion rate 25.0%; 95% CI, 11.4%–45.8%). Efficacy endpoints are reported in **Table 2**.

Available samples and analyses conducted at each timepoint are summarized in Supplementary Fig. S3.

PAM50 subtypes were as follows: LumB 56% ($n = 24$), LumA 25% ($n = 11$), and Basal 19% ($n = 8$). The pCR rate was significantly higher for Basal (50%) as compared with other subtypes (LumA 9%, LumB 8%; $P = 0.017$; **Fig. 2A**; Supplementary Fig. S4). The following inflammatory response and immune gene signatures were significantly overexpressed in pCR as compared with non-pCR patients (adjusted $P < 0.05$): CD8 T cells, cytotoxic cells, cytotoxicity, IFN gamma, inflammatory chemokines, macrophages, PD-L1, PD-L2, *IDO1*, TIGIT (T-cell immunoreceptor with immunoglobulin and ITIM domain), and tumor inflammation signature (**Fig. 2B**; Supplementary Fig. S4). Three gene signatures were significantly downregulated in pCR vs. non-pCR patients (adjusted $P < 0.05$): *FOXA1*, progesterone receptor, and androgen receptor, all tracking hormone receptor pathways (**Fig. 2B**; Supplementary Fig. S4). As a confirmation, progesterone receptor as evaluated by IHC was associated as a continuous variable to pCR (OR 0.97; 95% CI, 0.94–0.99, $P = 0.011$), whereas we found no association between continuous androgen receptor expression by IHC and pCR (OR, 0.99; 95% CI, 0.97–1.02, $P = 0.530$). There was a weak-to-moderate positive significant correlation of Basal subtype signature with each of the immune signatures that were significantly upregulated in pCR patients (Supplementary Fig. S5, Pearson coefficients ranging from 0.319 to 0.606). Of similar strength was the negative correlation of *FOXA1*, progesterone receptor, and androgen receptor signatures with the same immune-related signatures (Supplementary Fig. S5). These data suggest a partial biological overlap only between gene signatures tracking immunity and those related to intrinsic subtyping and hormone receptor pathways. Thus, we sought for how to integrate the contribution to pCR of these two biological areas.

To this aim, we considered TILs as a simple and easy-to-assess biomarker recapitulating the state of inflammation of the breast cancer microenvironment.

At t0, the median level of TILs in samples from patients achieving a pCR (15%; Q1:Q3, 4%:30%) was significantly higher as compared with non-pCR patients (2%; Q1:Q3, 1%:3%, $P < 0.001$; **Fig. 2C**).

We performed bivariate logistic regression analyses including TILs and a variable related to molecular subtyping. In the first model, both TILs and Basal subtype were independently associated with pCR (odds ratio, 1.16, 95% CI, 1.04–1.31, $P = 0.010$ for each 1% TIL increment, and odds ratio 10.71, 95% CI, 1.01–113.07, $P = 0.049$ for Basal vs. non-Basal subtype). The derived integrated score had an AUC of 0.95 (95% CI, 0.89–1.00) for pCR prediction (**Fig. 2D**). According to the optimal cutoff derived by receiving operator curve (ROC) analysis (1.74), pCR rate was 58.3% (7/12) versus 0% (0/31) for high vs low score ($P < 0.001$). In bivariate analyses combining TILs with either *FOXA1* signature, progesterone receptor signature, or androgen receptor signature, only TILs maintained an independent association with pCR (Supplementary Table S1).

Next, we characterized the immune infiltrate by mIHC. The lymphocyte infiltrate was mainly composed of $CD3^+$ T cells (median proportion of $CD3^+$ cells over total lymphocytes: 83.9%, Q1:Q3 74.5%:92.9%). The proportion of $CD4^+$ and $CD8^+$ cells among $CD3^+$ T lymphocytes was variable (median $CD4^+$ cells: 53.3%, Q1:Q3 30.8%:73.8%; median $CD8^+$ cells: 46.7%, Q1:Q3 26.2%:69.2%). PD-L1 was almost exclusively expressed by $CD68^+$ cells, whereas PD-1 expression was detected only on $CD3^+$ cells.

The intratumoral and stromal density of T lymphocytes ($CD3^+$; $P = 0.002$ and $P = 0.015$, respectively) and macrophages ($CD68^+$; $P = 0.016$ and $P = 0.005$, respectively), as evaluated by mIHC at t0, was higher in pCR versus non-pCR patients. A detailed analysis of immune cell subtypes and their functional states disclosed that pCR patients had higher intratumoral and stromal total $CD4^+$ cells ($P = 0.001$ and $P = 0.026$, respectively), higher intratumoral total $CD8^+$ cells ($P = 0.038$), intratumoral $CD4^+FoxP3^+$ T regulatory cells ($P = 0.002$), and stromal $CD68^+CD163^+$ tumor-associated macrophages ($P = 0.035$). The assessment of checkpoint molecule expression on immune cells revealed that both tumor regions, intratumoral and

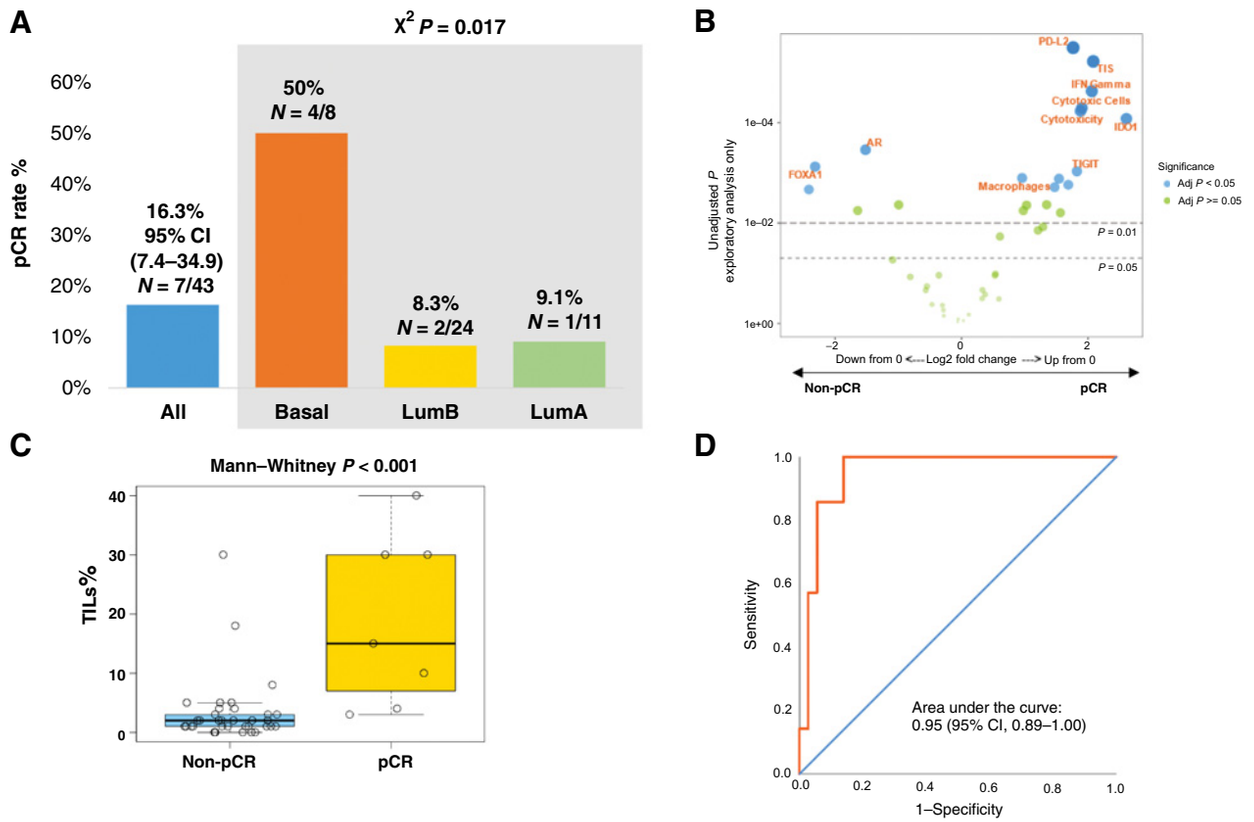

Figure 2.

Association of gene-expression parameters and TILs with pCR. **A,** Rate of pCR within different molecular intrinsic subtypes. **B,** Volcano plot showing differential expression of baseline gene-expression signatures assessed with the NanoString Breast Cancer 360 Panel in tumors achieving pCR as compared with tumors not achieving pCR. Displayed is the $\log_2$ fold difference in each gene-expression signature score between pCR and non-pCR. The gray dashed lines indicate the thresholds for unadjusted statistical significance ($P < 0.05$ and $P < 0.01$). Every dot represents one gene-expression signature. Blue dots represent gene signatures showing an association with pCR at the level of adjusted $P < 0.05$. **C,** Boxplot showing TIL levels in pCR vs. non-pCR patients. **D,** ROC showing the performance of the combined Basal subtype and TILs to predict pCR.

Table 2. Primary and secondary efficacy endpoints.

Efficacy endpoint	*N*/tot (%)	95% CI
pCR (ypT0/is, ypN0)	7/43 (16.3%)	7.4%–34.9%
RCB class 0–1	11/43 (25.6%)	14.0%–41.8%
Objective response by ultrasound (breast)[a]		
Complete	6/34 (17.6%)	7.4%–35.5%
Partial	18/34 (52.9%)	35.4%–70.7%
Complete or partial response	24/34 (70.6%)	52.3%–85.5%
Stable disease	7/34 (20.6%)	9.3%–38.8%
Progressive disease	3/34 (8.8%)	2.3%–25.0%
Breast-conserving surgery[b]	13/43 (30.2%)	17.7%–46.7%
Conversion from mastectomy to breast-conserving surgery	7/28 (25.0%)	11.4%–45.8%

Abbreviations: CI, confidence interval; *N*, number; pCR, pathologic complete response; RCB, residual cancer burden; tot, total.

[a]Calculated over a total of 34 patients who underwent breast ultrasound both at baseline and immediately before surgery. The remaining 9 patients underwent either breast MRI or contrast-enhanced mammography as per local policy and were not assessable for objective response according to protocol criteria.

[b]Reasons to perform mastectomy in 30 patients were: tumor size/breast volume ratio ($n = 17$), aesthetic reasons ($n = 3$), prophylactic procedure ($n = 3$), multicentric tumor ($n = 6$), and large calcification area ($n = 1$).

stromal, were characterized at t0 by higher densities of $CD3^+PD\text{-}1^+$ lymphocytes ($P < 0.001$ and $P = 0.004$, respectively), $CD68^+PD\text{-}L1^+$ ($P = 0.001$ and $P = 0.001$, respectively) and $CD68^+CD163^+PD\text{-}L1^+$ macrophages ($P = 0.001$ and $P < 0.001$, respectively) in pCR patients as compared with non-pCR counterparts. Data are shown in **Fig. 3A** and **B** (intratumoral compartment), and Supplementary Table S2 (intratumoral and stromal compartment). Analyses of mIHC immune markers at t1 in pCR versus non-pCR patients are also reported in Supplementary Table S2.

We also analyzed changes in immune cell populations from t0 to t1. TILs significantly increased after chemotherapy ($P = 0.029$; **Fig. 3C**). In the intratumoral compartment, a significant increase in total $CD8^+$ ($P = 0.009$) and $CD8^+$ granzyme B^+ ($P = 0.013$) cells was observed, whereas $CD4^+FoxP3^+$ and $CD68^+CD163^+$ cells significantly decreased in both the intratumoral ($P = 0.012$ and $P = 0.013$) and stromal ($P = 0.003$ and $P = 0.041$) compartments (**Fig. 3C** and **D**; Supplementary Fig. S6). As a confirmation of the shift in the tumor immune microenvironment, the $CD8^+/CD4^+$ ratio resulted higher at t1 versus t0 in both the intratumoral ($P = 0.003$) and stromal ($P = 0.008$) areas. Finally, we assessed the effect of nivolumab by analyzing changes from t1 to t2. Significant increases in intratumoral and stromal $CD8^+$ ($P < 0.001$ and $P = 0.039$), $CD8^+$ granzyme B^+ ($P = 0.018$ and $P = 0.024$), intratumoral $CD8^+/CD4^+$ ratio ($P = 0.040$), and stromal

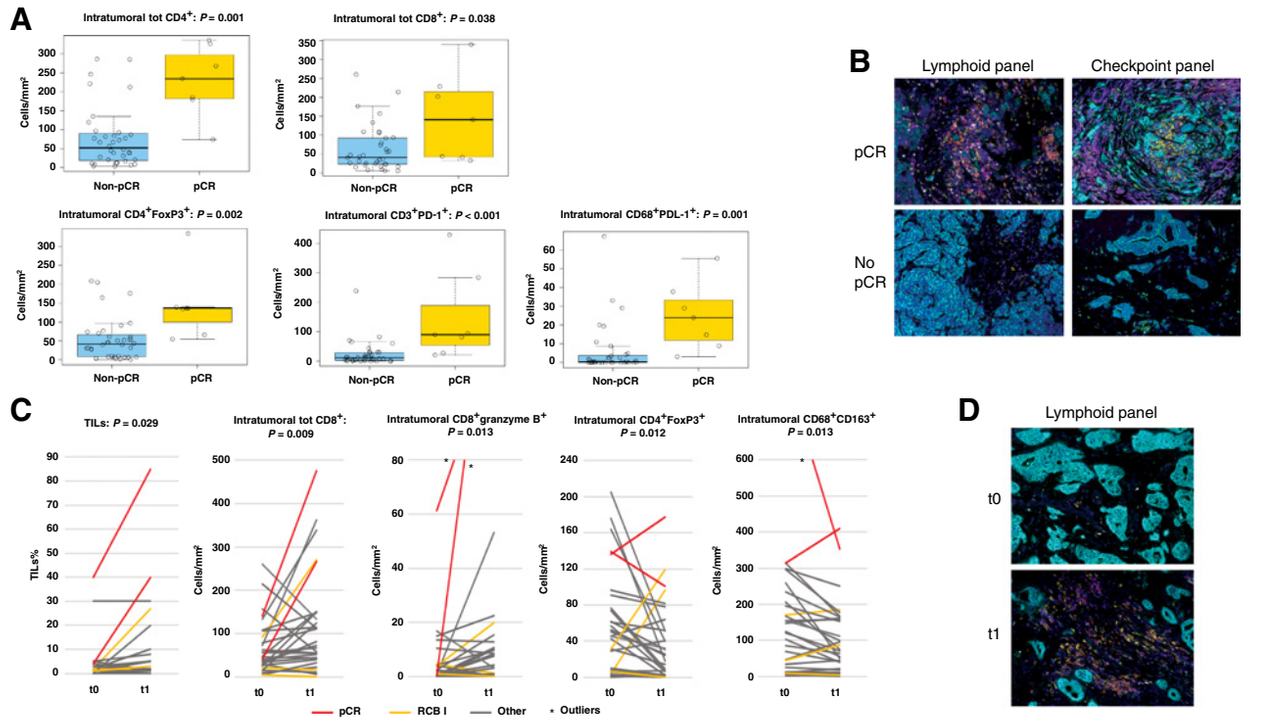

Figure 3.

A, Boxplots showing intratumoral immune cell populations by mIHC with significant different levels in pCR vs. non-pCR patients at t0. **B,** Representative pictures of mIHC staining at t0 in pCR and non pCR patients; original magnification 20×. **C,** Significant changes in TILs and intratumoral immune cell populations by mIHC from t0 to t1 in matched paired samples, with * indicating outlier values, red lines for patients with pCR, yellow lines for patients with RCB I, and gray lines for other patients. **D,** Representative pictures of a lymphoid mIHC panel at t0 and t1 from the same patient; original magnification 20×. Color code for mIHC pictures of checkpoint panel: CD3 in magenta, PD-1 in yellow, CD68 in white, CD163 in green, PD-L1 in red, pan-cytokeratin in cyan, nuclei in blue. Color code for mIHC pictures of lymphoid panel: CD8 in magenta, CD4 in yellow, granzyme B in green, FoxP3 in white, CD20 in orange, pan-cytokeratin in cyan, nuclei in blue.

$CD4^+$ granzyme B^+ ($P = 0.014$) were consistent with a checkpoint inhibitor–induced immune activation (Supplementary Fig. S6).

Table 3 summarizes TRAEs. During nivolumab, an increase in alanine aminotransferase (ALT, 33.3%), aspartate aminotransferase (AST, 31.0%), γ-glutamyltransferase (GGT, 19.0%), and arthralgia (21.4%, possibly related to concomitant endocrine therapy) represented the most common TRAEs of any grade. Increases in GGT (16.7%), ALT (16.7%), and AST (9.5%) accounted for the most common grade 3 TRAEs during nivolumab. Most frequent potentially immune-related adverse events during nivolumab were endocrinopathies (all grades 1–2), including hyperthyroidism (11.9%), hypothyroidism (14.3%), adrenal insufficiency (2.4%), and ACTH decrease (4.8%). Immune-related skin toxicities occurred in 5 patients, including one grade 3 erythema nodosum. One grade 3 immune-related pancreatitis was also observed. Serious adverse events during nivolumab were ALT and/or AST and/or GGT increase ($n = 3$), and immune-related pancreatitis ($n = 1$). Serious adverse events during chemotherapy included febrile neutropenia ($n = 2$).

Discussion

We reported the results of the first clinical trial of immunotherapy dedicated to patients with early HR-positive, HER2-negative breast cancer and the first study to incorporate both a molecular and an extensive immune cell infiltrate characterization by mIHC in LumB-like tumors.

The neoadjuvant sequential regimen of anthracycline-based chemotherapy followed by nivolumab and endocrine therapy was able to induce a pCR rate of 16.3% in LumB-like breast cancer patients. When considering residual cancer burden, 25.6% of patients were categorized as class 0 or 1. Objective responses in the breast were observed in 70.6% of evaluable patients.

The I-SPY2 adaptive trial is the only other study reporting data on neoadjuvant immunotherapy for HR-positive, HER2-negative breast cancer patients at high risk according to MammaPrint. The addition of pembrolizumab to the taxane component of a sequential taxane and anthracycline regimen graduated in this patients' subgroup with estimated pCR rates of 30% versus 13% with standard chemotherapy (22). Additional recent data from the same adaptive platform showed that the addition of durvalumab and olaparib to paclitaxel improved the pCR rate in HER2-negative breast cancer patients as compared with standard chemotherapy, especially in a subset of high-risk (defined by MammaPrint signature) HR-positive, HER2-negative breast cancer (estimated pCR 22% with control vs. 64% with durvalumab/olaparib; ref. 23). Comparison with the GIADA trial is limited by the I-SPY2 adaptive design, differences in chemotherapy backbone and treatment combinations, and differences in patient selection. However, the I-SPY2 results indicate that immunotherapy for patients with high-risk Luminal-like disease is worth exploring, supporting our background hypothesis.

The GIADA results compare favorably with data from recent trials dedicated to HR-positive HER2-negative breast cancer patients treated

Table 3. Summary of TRAEs.

	Chemotherapy phase, *n* = 43			
TRAEs occurring in >5% of patients (any grade)	**Any grade, *n* (%)**	**G1–2, *n* (%)**	**G3, *n* (%)**	**G4, *n* (%)**
Nausea	24 (55.8%)	24 (55.8%)	0	0
Neutropenia	16 (37.2%)	6 (14.0%)	6 (14.0%)	4 (9.3%)
Fatigue	15 (34.9%)	15 (34.9%)	0	0
Anemia	7 (16.3%)	7 (16.3%)	0	0
ALT increased	7 (16.3%)	5 (11.6%)	2 (4.7%)	0
White blood cells decreased	6 (14.0%)	4 (9.3%)	2 (4.7%)	0
GGT increased	5 (11.6%)	5 (11.6%)	0	0
AST increased	3 (7.0%)	2 (4.7%)	1 (2.3%)	0
Vomiting	3 (7.0%)	3 (7.0%)	0	0

	Nivolumab phase, *n* = 42			
TRAEs occurring in >5% of patients (any grade)	**Any grade, *n* (%)**	**G1–2, *n* (%)**	**G3, *n* (%)**	**G4, *n* (%)**
ALT increased	14 (33.3%)	7 (16.7%)	7 (16.7%)	0
AST increased	13 (31.0%)	9 (21.4%)	4 (9.5%)	0
Arthralgia	9 (21.4%)	9 (21.4%)	0	0
GGT increased	8 (19.0%)	1 (2.4%)	7 (16.7%)	0
Fatigue	5 (11.9%)	5 (11.95)	0	0
Anemia	4 (9.5%)	4 (9.5%)	0	0
Nausea	4 (9.5%)	4 (9.5%)	0	0
Lymphocyte count decreased	3 (7.1%)	2 (4.8%)	1 (2.4%)	0

	Nivolumab phase, *n* = 42			
Potentially irAEs (any incidence, any grade)	**Any grade, *n* (%)**	**G1–2, *n* (%)**	**G3, *n* (%)**	**G4, *n* (%)**
Hypothyroidism[a]	6 (14.3%)	6 (14.3%)	0	0
Hyperthyroidism[a]	5 (11.9%)	5 (11.9%)	0	0
Skin[b]	5 (11.9%)	4 (9.5%)	1 (2.4%)	0
ACTH decreased	2 (4.8%)	2 (4.8%)	0	0
Infusion-related reaction	2 (4.8%)	2 (4.8%)	0	0
Adrenal insufficiency	1 (2.4%)	1 (2.4%)	0	0
Pancreatitis	1 (2.4%)	0	1 (2.4%)	0

[a]Two patients had both hyperthyroidism and hypothyroidism.
[b]Including pruritus, maculopapular rash, acneiform rash, and erythema nodosum.

with standard anthracycline and taxane-based chemotherapy, showing pCR rates ranging from 5% to 10% (including data from patients with LumB breast cancer as defined by PAM50); nevertheless, the primary endpoint hypothesis was formally not satisfied (5, 24–27). The choice of an optimistic target was taken to counterbalance the risk of exposing patients to potential side effects in a curative setting. Indeed, we observed high rates of liver toxicity during nivolumab: Grade 3 ALT and AST increase occurred in 10% and 17% of patients, respectively, and grade 3 GGT increase occurred in 17% of patients. In the neoadjuvant phase III trials of immunotherapy for triple-negative breast cancer, the addition of pembrolizumab or atezolizumab to sequential taxanes and anthracyclines did not increase liver toxicity substantially, with grade ≥3 ALT and AST reported in around 5% of patients each (7, 8). The reasons for higher rates of liver function test abnormalities with nivolumab in GIADA are unclear and might be due to chemotherapy backbone, sequence and timing, role of endocrine therapy [although unlikely (28)], or simply by chance because of the small sample size.

Whichever the reason, this observation stresses the need for treatment personalization. Studies that are negative for their primary efficacy endpoint may generate precious translational data useful to plan more individualized treatment strategies.

Our trial population was enriched for patients with PAM50 LumB (56%) and Basal (19%) breast cancer as compared with other cohorts of HR-positive, HER2-negative breast cancer patients, probably as a result of the trial inclusion criteria (premenopausal patients, high grade and/or high Ki67; ref. 29). A high chemosensitivity is a well-known feature of Basal molecular subtype, with rates of pCR after neoadjuvant anthracycline and taxane-based chemotherapy of about 35% for Basal HR-positive, HER2-negative breast cancer (30). It is, however, unlikely that the increased chemosensitivity alone might account for the 50% pCR rate for Basal breast cancer observed in our trial, considering that patients received only 3 courses of epirubicin/cyclophosphamide as the initial segment of the planned treatment. Gene-expression data revealed the contribution of immune-related processes in the modulation of pCR. Even if, as expected, immune signatures were positively correlated with Basal subtype, the strength of the correlation was weak to moderate, suggesting that the biological information is not completely superimposable.

Consistent with gene-expression data, the simple evaluation of TILs on baseline tumor samples identified patients more likely to respond. TILs have been previously associated with response to neoadjuvant chemotherapy in HR-positive, HER2-negative breast cancer patients, with pCR rates of about 15% in case of TILs > 10% (31). With all the limitations of cross-study comparisons and potential biases related to patient selection, in our trial we observed a 71% pCR rate (5/7) for patients with TILs ≥ 10%.

We condensed the independent association of TILs and Basal subtype with pCR in a score that showed a high sensitivity and specificity for pCR prediction. Although this score should be further validated, our findings suggest that both biomarkers should be incorporated into the design of trials of chemoimmunotherapy for HR-positive, HER2-negative breast cancer.

We defined by mIHC a set of immune cell populations with significant higher levels in pCR versus non-pCR patients at baseline, including cytotoxic T cells, T regulatory cells, and immune checkpoint–expressing cells. Our data suggest that a proportion of LumB-like tumors displays an initial state of tumor inflammation counterbalanced by immunosuppressive elements, an immune profile that may define tumors more prone to respond to chemotherapy and immunotherapy sequence.

We also observed potential correlates of an immunogenic effect of anthracycline-based chemotherapy. After exposure to epirubicin–cyclophosphamide, we described an enrichment in TILs, intratumoral activated T cytotoxic cells, and a depletion of immunosuppressive cells. Our observations for early LumB-like breast cancer are consistent with the TONIC trial, showing that two low doses of doxorubicin turned the tumor immune microenvironment of metastatic triple-negative breast cancer into a more inflamed state (13). Finally, our data also suggest that exposure to nivolumab further enhanced the antitumor immune response in patients not achieving a pCR. Whether the immune infiltrate composition on residual disease after neoadjuvant chemotherapy has an impact on long-term prognosis deserves to be further investigated.

This study has limitations. It is a nonrandomized trial with a limited sample size; tissue samples at each timepoint were not evaluable for all included patients, and biomarker analyses were not corrected for multiplicity due to their exploratory nature. Therefore, the results must be considered as hypothesis-generating only. In our trial, it is impossible to fully disentangle the contribution of chemotherapy, immunotherapy, and endocrine therapy. However, the association between an increased expression of immune biomarkers and pCR rate revealed by translational analyses supports the initial hypothesis that the activity of the GIADA regimen as a whole is based on immune-related processes to a substantial extent. With regard to potential immunomodulatory effects of endocrine therapy, the observation of an increase in the $CD8^+/CD4^+$ T cells ratio from t1 to t2 is consistent with previous data comparing tumor samples before and after exposure to aromatase inhibitors. Relevant strengths include the study design; being the first study to test immunotherapy as part of the neoadjuvant treatment of HR-positive, HER2-negative breast cancer, the inclusion of a selected LumB-like population further dissected by molecular subtype and the integration of mIHC as part of the translational analyses.

In conclusion, although the study is formally negative, we reported an interesting rate of pCR and residual cancer burden class 0–1 with a sequence of anthracyclines and nivolumab combined with endocrine treatment for LumB-like breast cancer patients. Coupling clinical data with molecular and tissue-based biomarkers, we generate hypotheses that may contribute to change the way LumB-like is considered from an immunogenic perspective by identifying a subset of LumB-like breast cancer that could be particularly sensitive to chemotherapy and immunotherapy combinations, and by describing that the immune environment of LumB-like tumors might be modulated by treatment toward a more inflamed state.

Development of immunotherapy for early HR-positive, HER2-negative breast cancer is challenging. The risk of immune-related and long-term toxicities must be taken carefully into account in the light of generally good clinical outcomes for these patients. The identification of biomarkers potentially predictive of benefit from immunotherapy is crucial to guide proper patient selection. Ideally, future trials should be limited to HR-positive, HER2-negative breast cancer patients at higher risk of relapse and presenting with chemosensitive/immunogenic features as suggested by the GIADA and I-SPY 2 studies (i.e., Basal molecular subtype, high risk by MammaPrint, high immune infiltrate, high expression of immune signatures) and should evaluate the gain of a chemoimmunotherapy regimen as compared with standard chemotherapy. In this perspective, our results generate new hypotheses that, if validated, could trace the path of immunotherapy development in LumB-like breast cancer.

Authors' Disclosures

M.V. Dieci reports grants from BMS during the conduct of the study, as well as personal fees from Eli Lilly, Pfizer, Novartis, Seagen, Exact Sciences, and MSD outside the submitted work. V. Guarneri reports grants from BMS during the conduct of the study, as well as personal fees from Roche, Eli Lilly, Novartis, and MSD outside the submitted work. A. Musolino reports grants from Roche; grants and personal fees from Lilly; personal fees from Novartis and Seagen; personal fees and non-financial support from Macrogenics; and non-financial support from Pfizer outside the submitted work. S. Spazzapan reports other support from AstraZeneca, Daichii Sankyo, Eli Lilly, MSD, Novartis, Pfizer, and Tesaro outside the submitted work. G. Griguolo reports personal fees from Novartis and Eli Lilly, as well as non-financial support and other support from Pfizer, Novartis, Amgen, and Daichii Sankyo outside the submitted work. G.L. De Salvo reports grants from DISCOG–University of Padua during the conduct of the study. P. Conte reports grants and personal fees from Novartis, as well as personal fees from AstraZeneca outside the submitted work. No disclosures were reported by the other authors.

Authors' Contributions

M.V. Dieci: Conceptualization, resources, data curation, formal analysis, supervision, funding acquisition, investigation, writing–original draft, writing–review and editing. **V. Guarneri:** Conceptualization, resources, supervision, writing–review and editing. **A. Tosi:** Data curation, formal analysis, investigation, writing–original draft, writing–review and editing. **G. Bisagni:** Resources, data curation, writing–review and editing. **A. Musolino:** Resources, data curation, writing–review and editing. **S. Spazzapan:** Resources, data curation, writing–review and editing. **G. Moretti:** Resources, writing–review and editing. **G.M. Vernaci:** Resources, data curation, writing–review and editing. **G. Griguolo:** Resources, formal analysis, investigation, writing–review and editing. **T. Giarratano:** Resources, writing–review and editing. **L. Urso:** Data curation, investigation, writing–review and editing. **F. Schiavi:** Data curation, formal analysis, investigation, writing–review and editing. **C. Pinato:** Data curation, formal analysis, investigation, writing–review and editing. **G. Magni:** Data curation, formal analysis, writing–review and editing. **M. Lo Mele:** Resources, investigation, writing–review and editing. **G.L. De Salvo:** Data curation, formal analysis, methodology, writing–original draft, writing–review and editing. **A. Rosato:** Supervision, investigation, writing–original draft, writing–review and editing. **P. Conte:** Conceptualization, resources, supervision, funding acquisition, writing–review and editing.

Acknowledgments

The study was conceived and designed by the investigators from the University of Padova (P. Conte, M.V. Dieci, and V. Guarneri). Bristol Myers Squibb supplied nivolumab and funded the study but had no role in study design, data collection, data analysis, data interpretation, or writing of the report. The corresponding author had

full access to all data in the study and had final responsibility for the decision to submit for publication. The translational research was funded by Veneto Institute of Oncology IOV-IRCCS (5 per Mille 2017 grant to M.V. Dieci); Fondazione AIRC under IG 2018—ID. 21354 project—P.I. Rosato Antonio; 5 per Mille 2019—ID. 22759 program—G.L. Pierfranco Conte e G.L. Antonio Rosato; BIOV19ROSATO from 5 per Mille 2019, Veneto Institute of Oncology IOV-IRCCS to A. Rosato; and the Ministry of Health–Alliance Against Cancer (MoH-ACC) project "Research project on CAR T cells for hematological malignancies and solid tumors" to A. Rosato. Publication fees were supported by DiSCOG – Università di Padova "Bando Pubblicazioni 2021".

The publication costs of this article were defrayed in part by the payment of publication fees. Therefore, and solely to indicate this fact, this article is hereby marked "advertisement" in accordance with 18 USC section 1734.

Note

Supplementary data for this article are available at Clinical Cancer Research Online (http://clincancerres.aacrjournals.org/).

Received June 21, 2021; revised August 31, 2021; accepted October 12, 2021; published first October 19, 2021.

References

1. Viale G, Hanlon Newell AE, Walker E, Harlow G, Bai I, Russo L, et al. Ki-67 (30-9) scoring and differentiation of Luminal A- and Luminal B-like breast cancer subtypes. Breast Cancer Res Treat 2019;178:451–8.
2. Cardoso F, Kyriakides S, Ohno S, Penault-Llorca F, Poortmans P, Rubio IT, et al. Early breast cancer: ESMO Clinical Practice Guidelines for diagnosis, treatment and follow-up. Ann Oncol 2019;30:1194–220.
3. Cortazar P, Zhang L, Untch M, Mehta K, Costantino JP, Wolmark N, et al. Pathological complete response and long-term clinical benefit in breast cancer: the CTNeoBC pooled analysis. Lancet 2014;384:164–72.
4. von Minckwitz G, Untch M, Blohmer J-U, Costa SD, Eidtmann H, Fasching PA, et al. Definition and impact of pathologic complete response on prognosis after neoadjuvant chemotherapy in various intrinsic breast cancer subtypes. J Clin Oncol 2012;30:1796–804.
5. Gianni L, Mansutti M, Anton A, Calvo L, Bisagni G, Bermejo B, et al. Comparing neoadjuvant nab-paclitaxel vs paclitaxel both followed by anthracycline regimens in women with ERBB2/HER2-negative breast cancer—the evaluating treatment with neoadjuvant abraxane (ETNA) trial: a randomized phase 3 clinical trial. JAMA Oncol 2018;4:302–8.
6. Schmid P, Rugo HS, Adams S, Schneeweiss A, Barrios CH, Iwata H, et al. Atezolizumab plus nab-paclitaxel as first-line treatment for unresectable, locally advanced or metastatic triple-negative breast cancer (IMpassion130): updated efficacy results from a randomised, double-blind, placebo-controlled, phase 3 trial. Lancet Oncol 2020;21:44–59.
7. Schmid P, Cortes J, Pusztai L, McArthur H, Kümmel S, Bergh J, et al. Pembrolizumab for early triple-negative breast cancer. N Engl J Med 2020; 382:810–21.
8. Mittendorf EA, Zhang H, Barrios CH, Saji S, Jung KH, Hegg R, et al. Neoadjuvant atezolizumab in combination with sequential nab-paclitaxel and anthracycline-based chemotherapy versus placebo and chemotherapy in patients with early-stage triple-negative breast cancer (IMpassion031): a randomised, double-blind, phase 3 trial. Lancet 2020;396:1090–100.
9. Dieci MV, Griguolo G, Miglietta F, Guarneri V. The immune system and hormone-receptor positive breast cancer: is it really a dead end? Cancer Treat Rev 2016;46:9–19.
10. Criscitiello C, Vingiani A, Maisonneuve P, Viale G, Viale G, Curigliano G. Tumor-infiltrating lymphocytes (TILs) in ER+/HER2− breast cancer. Breast Cancer Res Treat 2020;183:347–54.
11. Luen S, Virassamy B, Savas P, Salgado R, Loi S. The genomic landscape of breast cancer and its interaction with host immunity. Breast 2016;29:241–50.
12. Anurag M, Zhu M, Huang C, Vasaikar S, Wang J, Hoog J, et al. Immune checkpoint profiles in luminal B breast cancer (alliance). J Natl Cancer Inst 2020; 112:737–46.
13. Voorwerk L, Slagter M, Horlings HM, Sikorska K, van de Vijver KK, de Maaker M, et al. Immune induction strategies in metastatic triple-negative breast cancer to enhance the sensitivity to PD-1 blockade: the TONIC trial. Nat Med 2019;25:920–8.
14. Apetoh L, Ghiringhelli F, Tesniere A, Obeid M, Ortiz C, Criollo A, et al. Toll-like receptor 4-dependent contribution of the immune system to anticancer chemotherapy and radiotherapy. Nat Med 2007;13:1050–9.
15. Generali D, Bates G, Berruti A, Brizzi MP, Campo L, Bonardi S, et al. Immunomodulation of FOXP3+ regulatory T cells by the aromatase inhibitor letrozole in breast cancer patients. Clin Cancer Res 2009;15:1046–51.
16. Huang H, Zhou J, Chen H, Li J, Zhang C, Jiang X, et al. The immunomodulatory effects of endocrine therapy in breast cancer. J Exp Clin Cancer Res 2021;40:19.
17. Parker JS, Mullins M, Cheang MCU, Leung S, Voduc D, Vickery T, et al. Supervised risk predictor of breast cancer based on intrinsic subtypes. J Clin Oncol 2009;27:1160–7.
18. Salgado R, Denkert C, Demaria S, Sirtaine N, Klauschen F, Pruneri G, et al. The evaluation of tumor-infiltrating lymphocytes (TILs) in breast cancer: recommendations by an International TILs Working Group 2014. Ann Oncol 2015;26: 259–71.
19. Bender R, Lange S. Adjusting for multiple testing—when and how? J Clin Epidemiol 2001;54:343–9.
20. Core Team R. R: a language and environment for statistical computing. 2017 [cited 2020 Oct 19]. Available at: https://www.R-project.org/.
21. Symmans WF, Wei C, Gould R, Yu X, Zhang Y, Liu M, et al. Long-term prognostic risk after neoadjuvant chemotherapy associated with residual cancer burden and breast cancer subtype. J Clin Oncol 2017;35:1049–60.
22. Nanda R, Liu MC, Yau C, Shatsky R, Pusztai L, Wallace A, et al. Effect of pembrolizumab plus neoadjuvant chemotherapy on pathologic complete response in women with early-stage breast cancer: an analysis of the ongoing phase 2 adaptively randomized I-SPY2 trial. JAMA Oncol 2020;6:676–84.
23. Pusztai L, Yau C, Wolf DM, Han HS, Du L, Wallace AM, et al. Durvalumab with olaparib and paclitaxel for high-risk HER2-negative stage II/III breast cancer: results from the adaptively randomized I-SPY2 trial. Cancer Cell 2021;39: 989–98.
24. Prat A, Saura C, Pascual T, Hernando C, Muñoz M, Paré L, et al. Ribociclib plus letrozole versus chemotherapy for postmenopausal women with hormone receptor-positive, HER2-negative, luminal B breast cancer (CORALLEEN): an open-label, multicentre, randomised, phase 2 trial. Lancet Oncol 2020;21:33–43.
25. Cottu P, D'Hondt V, Dureau S, Lerebours F, Desmoulins I, Heudel P-E, et al. Letrozole and palbociclib versus chemotherapy as neoadjuvant therapy of high-risk luminal breast cancer. Ann Oncol 2018;29:2334–40.
26. Yau C, Van Der Noordaa M, Wei J, Osdoit M, Reyal F, Hamy AS, et al. Abstract GS5–01: residual cancer burden after neoadjuvant therapy and long-term survival outcomes in breast cancer: a multi-center pooled analysis. Cancer Res 2020;80:GS5–01.
27. Esserman LJ, Berry DA, DeMichele A, Carey L, Davis SE, Buxton M, et al. Pathologic complete response predicts recurrence-free survival more effectively by cancer subset: results from the I-SPY 1 TRIAL–CALGB 150007/150012, ACRIN 6657. J Clin Oncol 2012;30:3242–9.
28. Francis PA, Pagani O, Fleming GF, Walley BA, Colleoni M, Láng I, et al. Tailoring adjuvant endocrine therapy for premenopausal breast cancer. N Engl J Med 2018;379:122–37.
29. Cejalvo JM, Pascual T, Fernández-Martínez A, Brasó-Maristany F, Gomis RR, Perou CM, et al. Clinical implications of the non-luminal intrinsic subtypes in hormone receptor-positive breast cancer. Cancer Treat Rev 2018;67:63–70.
30. Prat A, Fan C, Fernández A, Hoadley KA, Martinello R, Vidal M, et al. Response and survival of breast cancer intrinsic subtypes following multi-agent neoadjuvant chemotherapy. BMC Med 2015;13:303.
31. Denkert C, von Minckwitz G, Darb-Esfahani S, Lederer B, Heppner BI, Weber KE, et al. Tumour-infiltrating lymphocytes and prognosis in different subtypes of breast cancer: a pooled analysis of 3771 patients treated with neoadjuvant therapy. Lancet Oncol 2018;19:40–50.